Two nearly identical terpene synthases catalyze the formation of nerolidol and linalool in snapdragon flowers

Dinesh A. Nagegowda[1], Michael Gutensohn[2], Curtis G. Wilkerson[3] and Natalia Dudareva[1,*]

[1]*Department of Horticulture and Landscape Architecture, Purdue University, West Lafayette, IN 47907, USA,*
[2]*Institute of Biology – Plant Physiology, Martin-Luther-University Halle-Wittenberg, Weinbergweg 10, 06120 Halle/Saale, Germany, and*
[3]*Department of Energy Plant Research Laboratory and Michigan Proteome Consortium, Michigan State University, East Lansing, MI 48824, USA*

Summary

Terpenoids emitted from snapdragon flowers include three monoterpenes derived from geranyl diphosphate (GPP), myrcene, (*E*)-β-ocimene and linalool, and a sesquiterpene, nerolidol, derived from farnesyl diphosphate (FPP). Using a functional genomics approach, we have isolated and biochemically characterized two nearly identical nerolidol/linalool synthases, AmNES/LIS-1 and AmNES/LIS-2, two enzymes responsible for the terpenoid profile of snapdragon scent remaining to be characterized. The AmNES/LIS-2 protein has an additional 30 amino acids in the N-terminus, and shares 95% amino acid sequence identity with AmNES/LIS-1, with only 23 amino acid substitutions distributed across the homologous regions of the proteins. Although these two terpene synthases have very similar catalytic properties, and synthesize linalool and nerolidol as specific products from GPP and FPP, respectively, they are compartmentally segregated. GFP localization studies and analysis of enzyme activities in purified leucoplasts, together with our previous feeding experiments, revealed that AmNES/LIS-1 is localized in cytosol, and is responsible for nerolidol biosynthesis, whereas AmNES/LIS-2 is located in plastids, and accounts for linalool formation. Our results show that subcellular localization of bifunctional enzymes, in addition to the availability of substrate, controls the type of product formed. By directing nearly identical bifunctional enzymes to more than one cellular compartment, plants extend the range of available substrates for enzyme utilization, thus increasing the diversity of the metabolites produced.

Keywords: linalool, nerolidol, terpene synthases, floral volatiles, snapdragon.

Introduction

Terpenoids are the largest and most functionally and structurally diverse class of plant secondary metabolites. They are not only vital for numerous basic plant processes, such as photosynthesis, respiration, growth and development, but also for the fitness of a plant (Gershenzon and Kreis, 1999; Rodriguez-Concepcion and Boronat, 2002). Volatile terpenoids released from vegetative tissues defend plants against herbivore and pathogen attacks, and protect against reactive oxygen species, whereas their emission from flowers promotes plant–pollinator interactions (Dudareva et al., 2006). To date, 556 volatile terpenoids have been identified in the floral scent of many plant species, with monoterpenes representing the most abundant constitu-

ents, followed by sesquiterpenes, irregular terpenes and diterpenes (Knudsen and Gershenzon, 2006).

All terpenoids originate from isopentenyl diphosphate (IPP) and its allylic isomer dimethylallyl diphosphate (DMAPP), which are derived from two alternative pathways (Figure 1). In the cytosol, IPP is synthesized from acetyl-CoA (Newman and Chappell, 1999) by the mevalonic acid (MVA) pathway (McCaskill and Croteau, 1995), whereas in plastids, it is derived from pyruvate and glyceraldehyde-3-phosphate via the methyl-erythritol-phosphate (MEP) pathway (Lichtenthaler, 1999; Rohmer, 1999). Although the subcellular compartmentation allows these pathways to operate independently, metabolic 'crosstalk' between them was
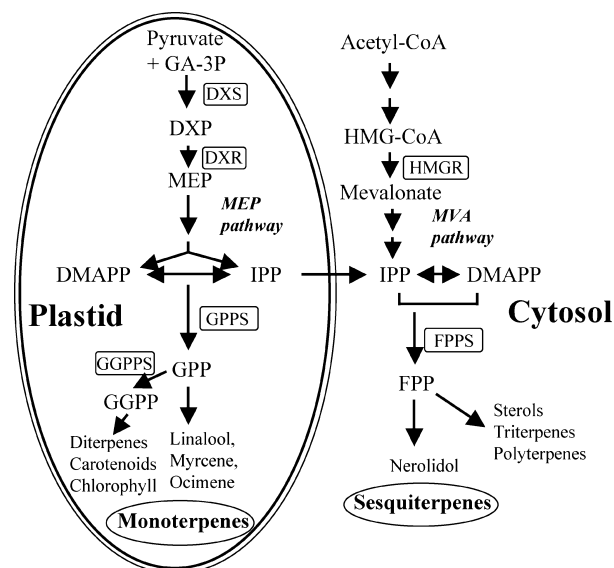
Figure 1. Metabolic pathways leading to terpenoid compound biosynthesis in snapdragon flowers.

Abbreviations: DMAPP, dimethylallyl diphosphate; DXP, 1-deoxy-D-xylulose-5-phosphate; DXR, DXP reductoisomerase; DXS, DXP synthase; FPP, farnesyl diphosphate; FPPS, FPP synthase; GA-3P, glyceraldehyde-3-phosphate; GGPP, geranylgeranyl diphosphate; GGPPS, GGPP synthase; GPP, geranyl diphosphate; GPPS, GPP synthase; HMG-CoA, 3-hydroxy-3-methylglutaryl-CoA; HMGR, 3-hydroxy-3-methylglutaryl-CoA reductase; IPP, isopentenyl diphosphate; MEP, 2-C-methyl-D-erythritol-4-phosphate; MVA, mevalonic acid. The solid arrow from the plastid to the cytosol shows trafficking of IPP in snapdragon (Dudareva *et al.*, 2005).

previously discovered (Schuhr *et al.*, 2003), particularly from plastids to the cytosol (Dudareva *et al.*, 2005; Hemmerlin *et al.*, 2003; Laule *et al.*, 2003).

In both subcellular compartments, prenyltransferases use IPP and DMAPP to produce prenyl diphosphates. In the cytosol, the condensation of two IPP molecules and one DMAPP molecule catalyzed by the enzyme farnesyl diphosphate synthase (FPPS) results in FPP formation (C_{15}), the natural precursor of sesquiterpenes (McGarvey and Croteau, 1995). In plastids, a head-to-tail condensation of one IPP molecule and one DMAPP molecule catalyzed by geranyl diphosphate synthase (GPPS) forms GPP (C_{10}), the universal precursor of all monoterpenes (Ogura and Koyama, 1998; Poulter and Rilling, 1981). Condensation of one DMAPP molecule with three IPP molecules by the action of geranylgeranyl diphosphate synthase (GGPPS) yields GGPP, the C_{20} diphosphate precursor of diterpenes (Koyama and Ogura, 1999). Following the formation of the acyclic precursors GPP, FPP and GGPP, a wide range of structurally diverse cyclic and acyclic monoterpenes, sesquiterpenes and diterpenes is generated through the action of a large family of terpene synthases/cyclases (TPSs; Cane, 1999; Wise and Croteau, 1999).

Snapdragon flowers emit three monoterpenes derived from GPP, myrcene, (*E*)-β-ocimene and linalool, as well as

the sesquiterpene (*E*)-nerolidol, derived from FPP (Dudareva *et al.*, 2003, 2005). Emission of these compounds follows diurnal rhythms, and is controlled by a circadian clock. Two specialized monoterpene synthases responsible for synthesizing myrcene and (*E*)-β-ocimene, respectively, have been isolated and functionally characterized (Dudareva *et al.*, 2003). However, there is no information about linalool and nerolidol biosynthesis in snapdragon flowers. The formation of these compounds could follow at least two scenarios, and require two specialized TPSs, linalool synthase and nerolidol synthase, or be the result of the action of a bifunctional nerolidol/linalool synthase, as was recently reported in strawberry (Aharoni *et al.*, 2004). It was also proposed that linalool biosynthesis in ripe strawberry fruit occurs in the cytosol (Aharoni *et al.*, 2004; Hampel *et al.*, 2006), in contrast to the generally accepted plastidial origin of monoterpenes, thereby questioning the subcellular compartmentalization of linalool formation in the petal tissue of snapdragon flowers. Here, we show that snapdragon possesses two nearly identical bifunctional TPSs, which are responsible for linalool and nerolidol biosynthesis in flowers. Biosynthesis of these compounds is compartmentally separated, with linalool biosynthesis occuring in plastids and nerolidol biosynthesis occuring in the cytosol. Our results also provide evidence that the subcellular localization of the enzyme and the availability of the substrate determine the type of product formed.

Results

Isolation of terpene synthase genes responsible for linalool and nerolidol biosynthesis in snapdragon flowers

A search of a snapdragon expressed sequence tag (EST) database, containing >25 000 random sequences from different plant organs (Bey *et al.*, 2004), for clones with sequence similarity to known TPSs resulted in five contigs corresponding to transcripts of two similar genes. Two clones, *ama1i06* and *ama2j20*, designated as AmNES/LIS-1 and AmNES/LIS-2 (for *Antirrhinum majus* nerolidol/linalool synthase; see below), respectively, represent full-length cDNAs of 1885 and 1898 nucleotides, and share 97% identity. These cDNAs encode proteins of 566 and 596 amino acids (aa), with calculated molecular weights of 65 218 and 68 466 Da, respectively (Figure 2a). The protein encoded by AmNES/LIS-2 has an additional 30 aa in its N-terminus, and shares 95% aa sequence identity with AmNES/LIS-1. Both proteins exhibit ∼62% aa identity to snapdragon myrcene and (*E*)-β-ocimene synthases, as well as ∼50% and 43% identity to strawberry nerolidol/linalool synthases (Aharoni *et al.*, 2004) and Arabidopsis linalool synthase (Chen *et al.*, 2003), respectively (Figure 2a). Like other monoterpene synthases from snapdragon, AmNES/LIS proteins belong to the *TPS-g* subfamily (Figure 2b; Dudareva *et al.*, 2003),

which lacks the RRx$_8$W motif, a key feature of all monoterpene synthases of the *Tps-b* and *Tps-d* groups (Aubourg *et al.*, 2002; Bohlmann *et al.*, 1998b).

Functional characterization of snapdragon AmNES/LIS proteins

For functional characterization of AmNES/LIS proteins, the coding region of each gene was subcloned into an expression vector, and encoded proteins were expressed in *Escherichia coli* and analyzed for TPS activities. Although the crude bacterial extract containing AmNES/LIS-1 protein showed activity with both GPP and FPP, no activity was found in AmNES/LIS-2. The absence of activity could be caused by inclusion body formation as a result of transit peptide presence, a typical feature of monoterpene synthases (Bohlmann *et al.*, 1998b; Williams *et al.*, 1998). Although *in silico* analysis of the AmNES/LIS-2 N-terminal sequence did not give a clear indication of the presence of a transit peptide, truncations were made before the second (Met-31) and third (Met-79) methionines (indicated by arrowheads in Figure 2a), and the corresponding proteins were expressed in *E. coli*. As both truncated AmNES/LIS-2 proteins efficiently converted GPP and FPP to products, it is possible that the N-terminal 30 aa are responsible for inclusion body formation.

Recombinant purified AmNES/LIS-1, Met-31-AmNES/LIS-2 and Met-79-AmNES/LIS-2 proteins predominantly catalyzed the formation of linalool from GPP (Figure 3a,c, data for Met-79-AmNES/LIS-2 not shown), and of (*E*)-nerolidol from FPP (Figure 3b,d). In addition, trace levels of (*E*)-β-ocimene (<1%), myrcene (<0.5%) and α-pinene (<0.15%) were formed from GPP, and β-farnesene (<0.4%), α-farnesene (<0.3%) and α-bisabolol (<0.12%) were formed from FPP. To determine the absolute configuration of linalool and nerolidol produced by AmNES/LIS proteins as well as snapdragon flowers, enantioselective GC-MS analysis was performed. Both enzymes exclusively synthesized (*S*)-linalool from GPP (Figure 4c,e) and (*3S*)(*E*)-nerolidol from FPP (Figure 4d,f), with the same conformation of terpenoids found for both in the scent of the flower (Figure 4g,h).

To test for the presence of nerolidol and linalool synthase activities in snapdragon, crude protein extracts from upper and lower petal lobes of 5-day-old flowers, a developmental stage with the highest terpenoid emission (Dudareva *et al.*, 2003), were assayed with GPP and FPP. GC-MS analysis revealed that the sesquiterpene (*E*)-nerolidol was produced upon incubation with FPP (Figure 5b), whereas three monoterpenes, linalool (12.9% of total product), (*E*)-β-ocimene (71.9%) and myrcene (9.3%), along with minor quantities of (*Z*)-β-ocimene, were formed from GPP (Figure 5a).

Biochemical characterization of purified recombinant AmNES/LIS1 and Met-31-AmNES/LIS-2 proteins revealed that they exhibit similar properties and require, for activity, a divalent cation co-factor, Mg^{2+} or Mn^{2+}. Both linalool and nerolidol synthase activities showed a preference for Mg^{2+}, and were 2.9- and 6.7-fold higher in the presence of Mg^{2+} than Mn^{2+}, respectively. Mn^{2+} inhibited corresponding activities by 44% and 70%, respectively, in the presence of Mg^{2+} (6 mm). Although maximum TPS activity was achieved at 2.0–8.0 mm Mg^{2+}, further increases in Mg^{2+} to 20 mm led to a 20% reduction in the maximum velocity. The apparent K_m values for Mg^{2+} were 1.16 and 1.06 mm in the presence of GPP, and 0.32 and 0.34 mm in the presence of FPP, for AmNES/LIS-1 and AmNES/LIS-2, respectively (Table 1).

AmNES/LIS proteins were active over a broad range of pH values from 5.0 to 9.0, with maximum activity at pH 8.0. The molecular mass of 66.1 kDa for the recombinant AmNES/LIS-1 was determined by gel filtration chromatography, and was consistent with the predicted molecular mass (65.2 kDa), indicating that the active enzyme is a monomer. Kinetic characterization of AmNES/LIS-1 and AmNES/LIS-2 using a range of FPP (3–110 μm) and GPP (2–65 μm) concentrations resulted in very similar apparent K_m values of 7.57 and 7.68 μm for GPP, and 24.13 and 22.68 μm for FPP, respectively (Table 1). Both enzymes show similar catalytic efficiencies (k_{cat}/K_m ratio) with GPP, which were slightly lower than with FPP (Table 1).

Identification of AmNES/LIS in snapdragon flowers

To verify the involvement of AmNES/LIS enzymes in linalool and (*E*)-nerolidol formation in snapdragon flowers, proteins were partially purified from petal lobes of 4- to 6-day-old flowers using several chromatographic steps. As AmNES/LIS proteins use GPP and FPP as substrates, fractions during purification were analyzed for both monoterpene and sesquiterpene synthase activities, which we were unable to separate, as they eluted together. Three final fractions with the highest TPS activities were combined and run on SDS-PAGE, which revealed a single protein band of ∼60 kDa. (Figure S1). Protein sequencing of this band and surrounding proteins within 1 cm by LC-MS/MS, followed by screening a snapdragon EST database comprising >25 000 sequences, revealed six peptides corresponding to the predicted AmNES/LIS protein sequences, and fourteen peptides matching the protein sequences of the previously characterized myrcene and ocimene synthases (Dudareva *et al.*, 2003). No peptides corresponding to other TPSs were found in the sequencing output, providing clear evidence that these TPSs are responsible for terpenoid emission in snapdragon flowers.

Subcellular localization of AmNES/LIS proteins

The biochemical characterization of AmNES/LIS proteins showed that they can potentially participate in linalool formation, a process that is believed to take place in the
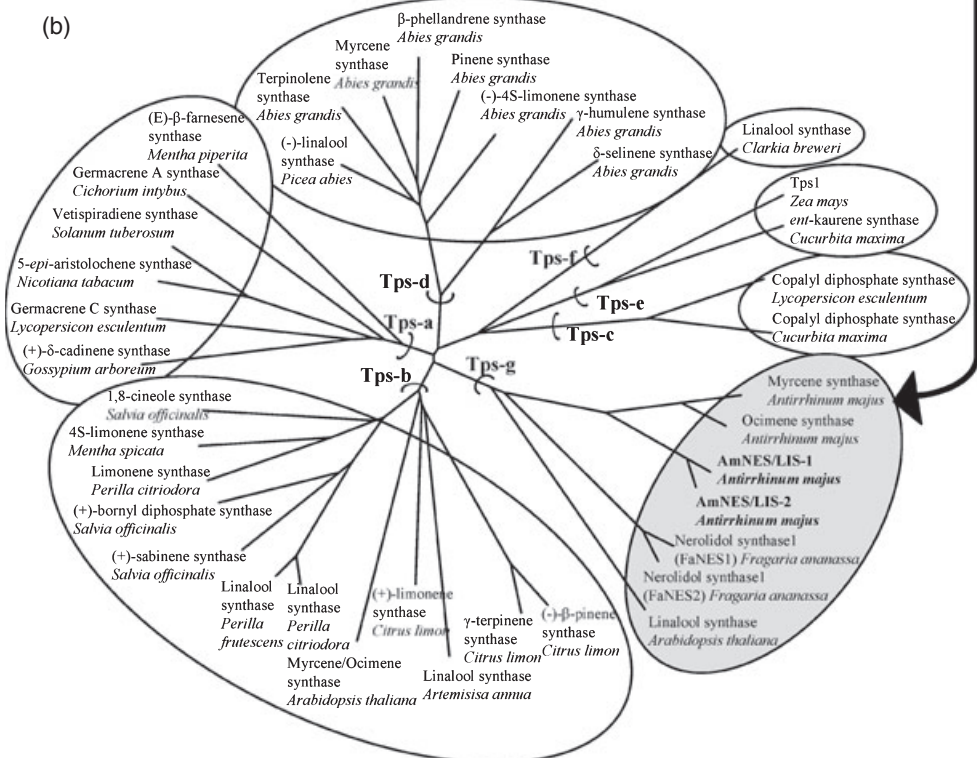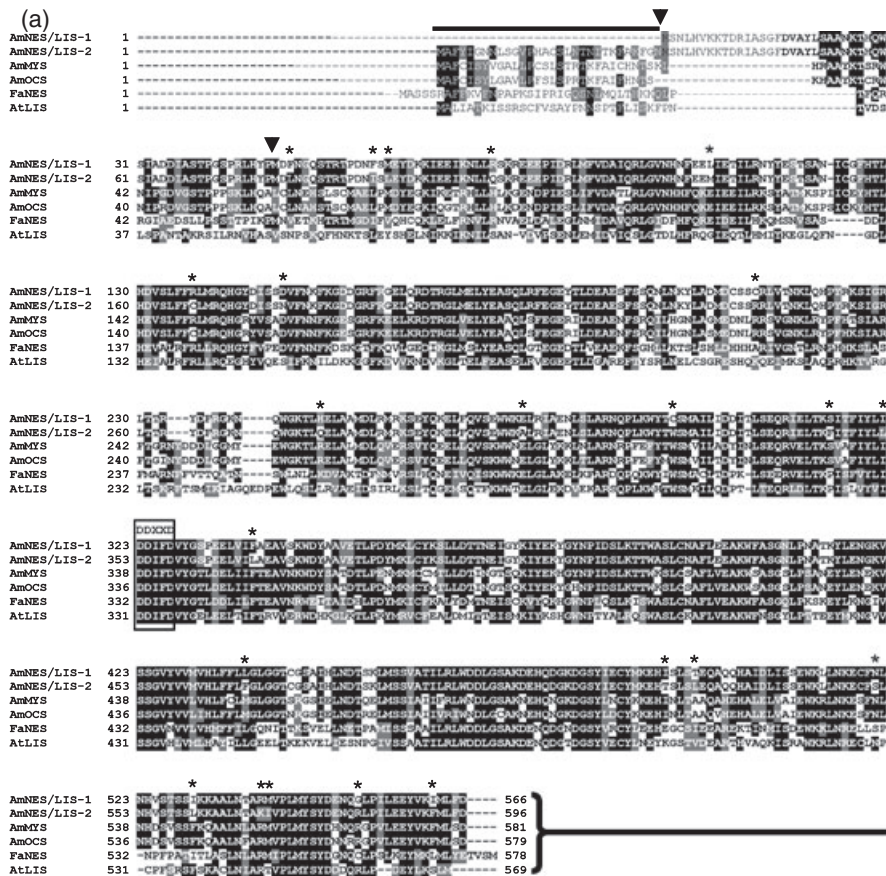
(a)

(b)

Figure 2. Relatedness of AmNES/LIS proteins to other terpene synthases.
(a) Alignment of AmNES/LIS-1 (GenBank accession no. EF433761) and AmNES/LIS-2 (GenBank accession no. EF433762) predicted amino acid sequences with snapdragon myrcene synthase (AAO41726), (*E*)-β-ocimene synthase (AAO42614), strawberry nerolidol/linalool synthase (FaNES; CAD57106) and Arabidopsis linalool synthase (AAO85533). The alignment was performed using CLUSTALW, and was shaded with BoxShade version 3.21 software (Human Genome Sequencing Center, http://www.hgsc.bcm.tmc.edu). Residues in black are conserved (identical in at least four out of six sequences shown), whereas residues in gray are similar in at least two of the six sequences shown. Dashes indicate gaps inserted for optimal alignment. The horizontal line indicates the N-terminal peptide, which was shown to be involved in AmNES/LIS-2 protein targeting to plastids. The conserved DDxxD motif is shown in the box. Arrowheads indicate positions of Met-31 and Met-79 in AmNES/LIS-2 where truncations were made. Asterisks show 23 amino acid differences between AmNES/LIS-1 and AmNES/LIS-2.
(b) Phylogenetic tree illustrating AmNES/LIS-1 and AmNES/LIS-2 as members of the *Tps-g* subfamily. Subfamilies are divided based on cluster analysis (Aubourg *et al.*, 2002; Bohlmann *et al.*, 1998b). The unrooted neighbor-joining tree was created using CLUSTALX and TREEVIEW for visualization. Only a subset of the known plant terpene synthases (TPSs) is shown: *Artemisia annua* linalool synthase (AAF13356); *Abies grandis* (−)-4*S*-limonene synthase (AF006193), myrcene synthase (U87908), pinene synthase (U87909), terpinolene synthase (AF139206), β-phellandrene synthase (AF139205), γ-humulene synthase (U92267) and δ-selinene synthase (U92266); *Arabidopsis thaliana* myrcene/ocimene synthase (AF178535); *Clarkia breweri* linalool synthase (U58314); *Cichorium intybus* germacrene A synthase (AF497999); *Citrus limon* (−)-β-pinene synthase (AF514288), (+)-limonene synthase (AF514287) and γ-terpinene synthase (AF514286); *Cucurbita maxima* copalyl diphosphate synthase (AF049905) and *ent*-kaurene synthase (U43904); *Gossypium arboreum* (+)-δ-cadinene synthase (U23205); *Lycopersicon esculentum* copalyl diphosphate synthase (AB015675) and germacrene C synthase (AF035630); *Mentha piperita* (*E*)-β-farnesene synthase (AF024615); *Mentha spicata* 4*S*-limonene synthase (L13459); *Nicotiana tabacum* 5-*epi*-aristolochene synthase (L04680); *Picus abies* linalool synthase (AAS47693); *Perilla citridora* limonene synthase (AF241790) and linalool synthase (AY917193); *Perilla frutescens* linalool synthase (AF444798); *Salvia officinalis* (+)-bornyl diphosphate synthase (AF051900), (+)-sabinene synthase (AF051901) and 1,8-cineole synthase (AF051899); *Solanum tuberosum* vetispiradiene synthase (AB022598); *Zea mays* TPS1 (AAO18435).

plastids, based on the presence of a transit peptide in the protein (Crowell *et al.*, 2002; Jia *et al.*, 1999), or in the cytosol, as was proposed in strawberry through labeling experiments (Hampel *et al.*, 2006). To determine the site of linalool biosynthesis in snapdragon, leucoplasts were purified from petal lobes of 5-day-old flowers (Figure 5c,d), and were assayed with GPP. The isolated leucoplasts were free from cytosolic contamination, as assessed using marker enzyme assays specific for subcellular compartments (Figure S2), and did not contain detectable levels of linalool and nerolidol prior to the addition of prenyl diphosphate substrates. GC-MS analysis of the products revealed that linalool was one of the monoterpenes produced from supplied GPP (Figure 5e), suggesting that it is made in plastids.

Software (CHLOROP, http://www.cbs.dtu.dk/services/-ChloroP; TARGETP, http://www.cbs.dtu.dk/services/TargetP; PWOLF PSORT, http://wolfpsort.seq.cbrc.jp; PREDOTAR, http://urgi.versailles.inra.fr/predotar; SIGNALP, http://www.-cbs.dtu.dk/services/SignalP) was used to predict the likelihood of targeting signals in the N-termini of AmNES/LIS proteins. Based on all program predictions, AmNES/LIS-1 did not contain a targeting signal and was localized in the cytosol. However, no consistent conclusions could be drawn about the subcellular localization of AmNES/LIS-2, as three of the search algorithms predicted its cytosolic localization, whereas the CHLOROP and PREDOTAR programs predicted the presence of a plastid-targeting sequence with 49% and 77% probability, respectively. To experimentally determine the subcellular localization of AmNES/LIS proteins, coding regions of each gene were fused to a GFP reporter gene, and were then transferred to Arabidopsis protoplasts, where corresponding transient GFP expression was analyzed by confocal laser scanning microscopy (Figure 6). GFP fluorescence was observed in the cytosol of protoplasts expressing AmNES/LIS-1-GFP (Figure 6e–l), confirming AmNES/LIS-1 cytosolic localization.

Unlike AmNES/LIS-1-GFP, the AmNES/LIS-2-GFP fusion protein exhibited a punctate and discrete pattern associated with the chloroplasts (Figure 6m–t), indicating its plastidial location. Elimination of the first 30 aa in AmNES/LIS-2 changed the subcellular localization of the protein from plastid to cytosol (Figure 6u–b1). When the first 30 aa of AmNES/LIS-2 were fused to GFP, the fluorescence was detected only in the cytosol (data not shown), suggesting that these 30 aa are essential but not sufficient for targeting the protein to the chloroplast. However, when the first 69 aa of this protein were fused to GFP, the GFP was directed to chloroplasts, and its fluorescence was localized evenly throughout the plastids (Figure 6c1–j1). The pattern of accumulation of the 69-aa$_{(AmNES/LIS-2)}$-GFP in chloroplasts resembled that of GFP fused to the transit peptide of RuBisCO small subunit, which is a stromal protein (Figure 6k1–n1). These results clearly show that the AmNES/LIS-2 protein contains a transit peptide that mediates its chloroplast targeting. *In vitro* protein import experiments further confirmed the subcellular localization of AmNES/LIS proteins (data not shown).

As AmNES/LIS-2 is localized in plastids and can catalyze the formation of both linalool and nerolidol (Figure 3c,d), we checked the presence of sesquiterpene synthase activity in leucoplasts. Purified leucoplasts produced nerolidol from FPP (Figure 5f), suggesting that in addition to linalool synthase activity (Figure 5e), nerolidol synthase activity exists in plastids. Both activities were also found in the cytosol.

Analysis of expression of AmNES/LIS-1 *and* AmNES/LIS-2 *genes*

The mRNA expression of AmNES/LIS genes was analyzed in different floral tissues and petals during flower development by quantitative real-time PCR with gene-specific primers.
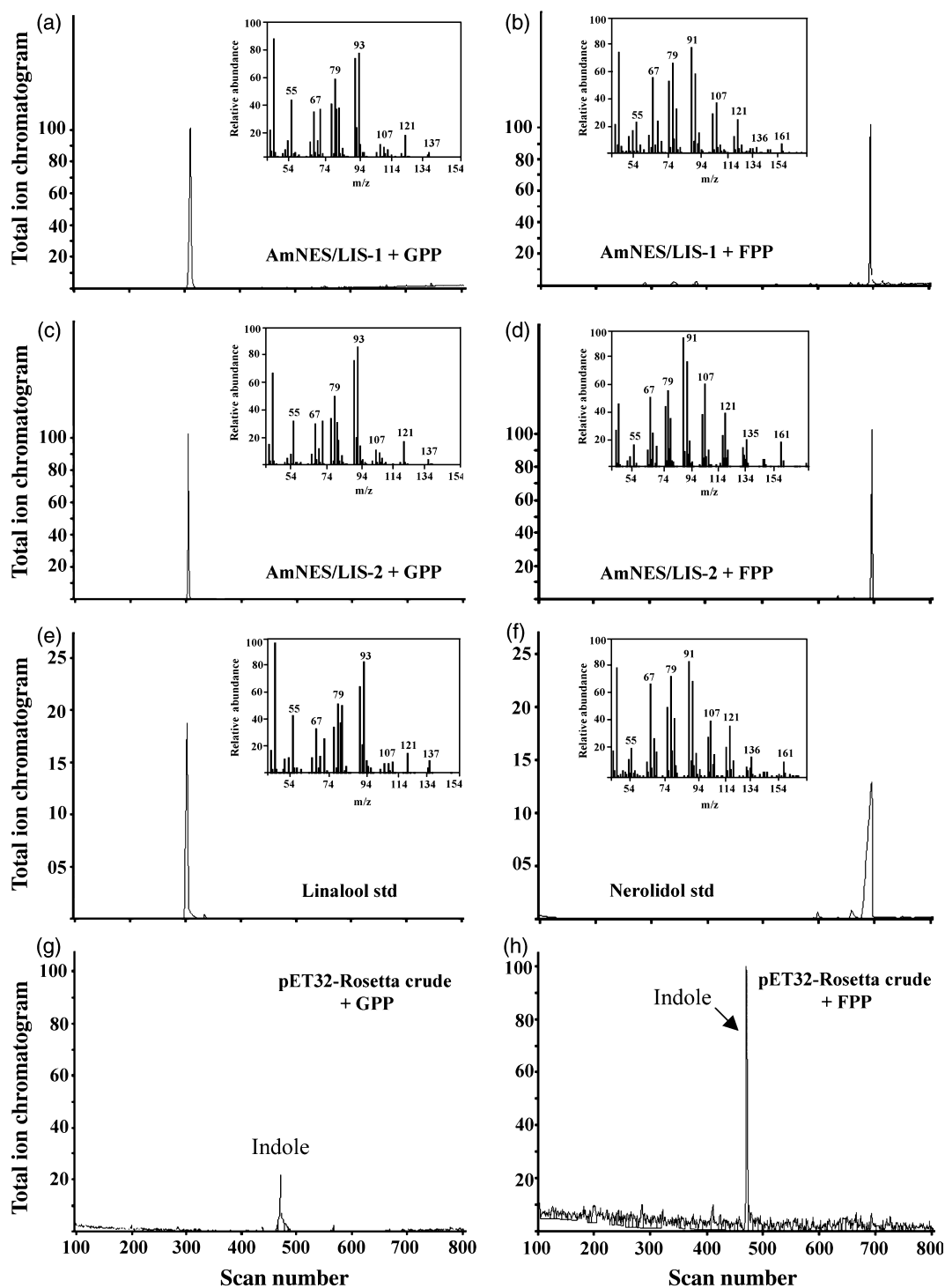
Figure 3. Analyses of products formed by AmNES/LIS enzymes from geranyl diphosphate (GPP) and farnesyl diphosphate (FPP).

(a–f) GC-MS analysis of products formed by recombinant AmNES/LIS-1 (a, b) and AmNES/LIS-2 (c, d) from GPP (a, c) and FPP (b, d), respectively. Reaction products were obtained by solid-phase microextraction (SPME). Inserts with numbered peaks in a–f represent mass spectra of corresponding products. Retention times and mass spectra of synthesized linalool (a, c) and nerolidol (b, d) are identical to those of corresponding authentic standards (e, f, respectively); *m/z*, mass-to-charge ratio.

(g, h) GC-MS chromatograms of the products formed by extracts of *Escherichia coli* expressing the pET-32 vector without an insert (control) in the presence of GPP (g) and FPP (h), respectively.

Figure 4. Chiral analysis of linalool and nerolidol emitted by snapdragon flowers and formed by AmNES/LIS enzymes.

(a, b) Racemic mixtures of linalool and nerolidol. Peaks 1 and 2, (*3R*)- and (*3S*)(*Z*)-nerolidol (the elution order is unknown); peaks 3 and 4, (*3R*)- and (*3S*)(*E*)-nerolidol, respectively.

(c, e) (*S*)-linalool produced by AmNES/LIS-1 (c) and AmNES/LIS-2 (E) from GPP.

(d, f) (*3S*)-(*E*)-nerolidol produced by AmNES/LIS-1 (d) and AmNES/LIS-2 (f) from FPP.

(g, h) (*S*)-linalool and (*3S*)-(*E*)-nerolidol emitted by snapdragon flowers.
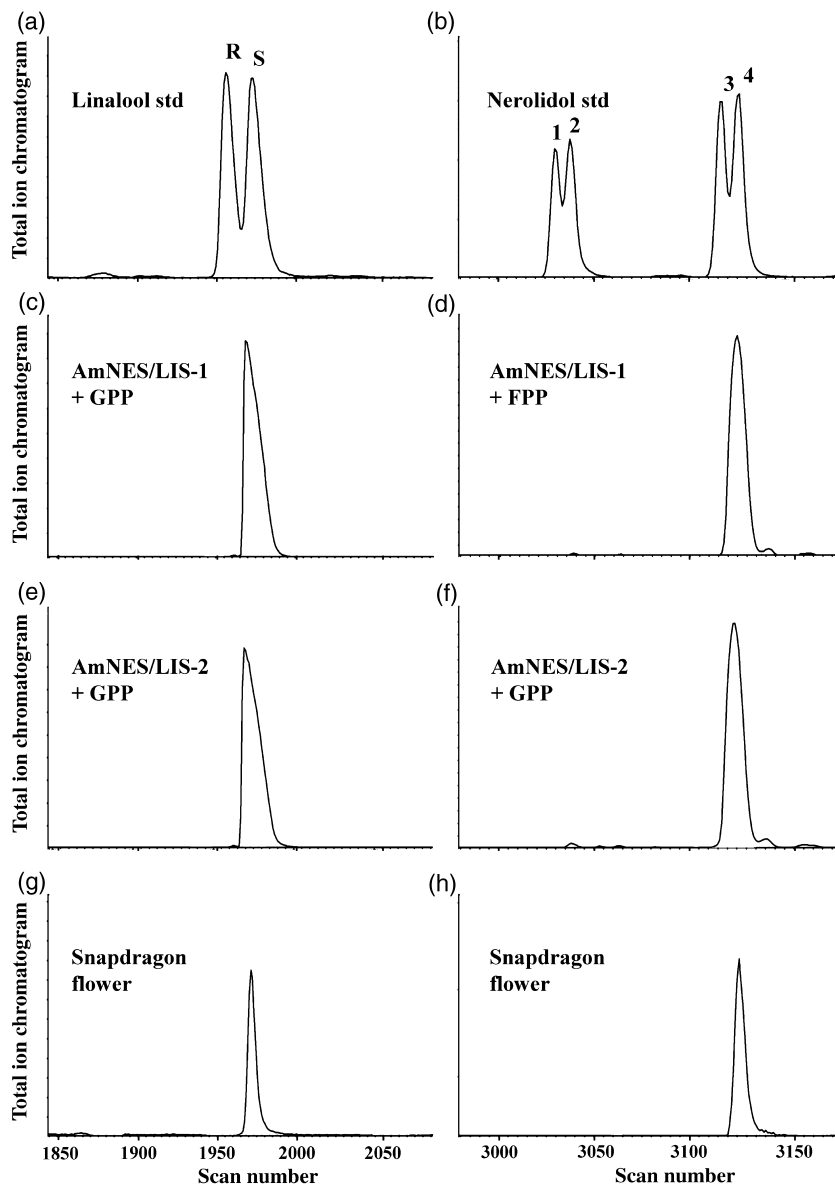
The expression of both genes was highest in the upper and lower petal lobes (Figure 7a), which are the parts of the flower that have previously been shown to be primarily responsible for scent emission in snapdragon (Dudareva *et al.*, 2000, 2003). *AmNES/LIS* transcripts were also detected at lower levels in tubes, followed by pistils, stamens and ovaries (Figure 7a). A negligible level of transcripts was found in leaves and sepals.

During flower development, mRNA levels for both genes in petal lobes gradually increased during the first 3 or 4 days, peaking on days 3 and 5 postanthesis for *AmNES/LIS-2* and *AmNES/LIS-1*, respectively, and they remained relatively stable thereafter for *AmNES/LIS-2*, but slightly decreased for *AmNES/LIS-1* (Figure 7b). TPS activities in petal lobes were also developmentally regulated. Nerolidol synthase activity

peaked on day 5 and decreased by 50% in old flowers (10–12 days postanthesis), whereas linalool synthase activity peaked on day 5 and remained stable (Figure 7c). Emission of linalool and nerolidol positively correlated with the corresponding TPS activities ($P < 0.0001$ for both activities) only in young flowers, in which emission of both compounds peaked sharply on day 5–6 postanthesis (Figure 7d). Although the positive correlation between linalool synthase activity and *AmNES/LIS-2* transcript abundances was observed over the entire flower development, nerolidol synthase activity correlated with *AmNES/LIS-1* expression only up to day 9 postanthesis (Figure 7b,c). These results suggest that regulation of enzyme activities occurs largely at the level of gene expression, and, in the case of nerolidol synthase activity, post-transcriptional or translational/
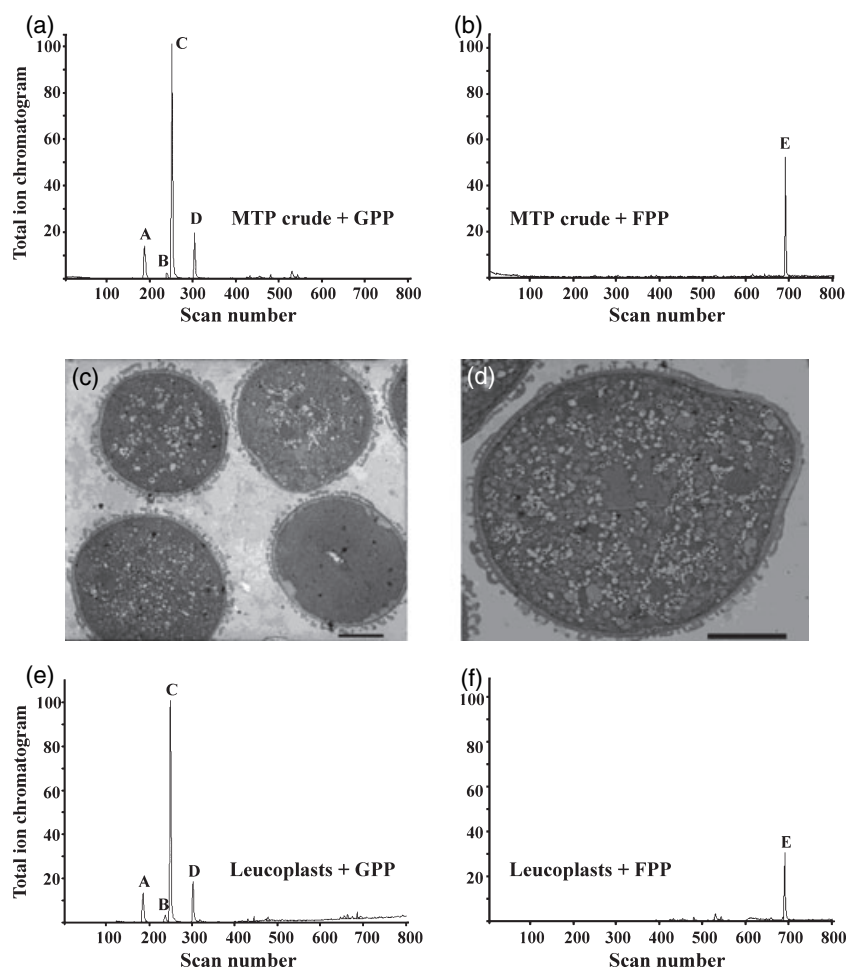
Figure 5. Products formed by snapdragon petal crude extracts and purified leucoplasts from geranyl diphosphate (GPP) and farnesyl diphosphate (FPP).
Solid-phase microextraction (SPME)-gas chromatographs of products formed from GPP (a) and FPP (b) by petal crude extracts of 5-day-old flowers. Scanning electron microscopy of purified leucoplasts (c and d). Scale bars: 0.5 μm (c, d). SPME-gas chromatographs of products produced from GPP (e) and FPP (f) by purified leucoplasts. Peaks are myrcene (a), (Z)-β-ocimene (b), (E)-β-ocimene (c), linalool (d) and nerolidol (e).

Table 1 Kinetic parameters of AmNES/LIS proteins

Gene	Substrate	K_m (μM)	V_{max} (pcat mg^{-1})	k_{cat} (sec^{-1})	k_{cat}/K_m (mM^{-1} sec^{-1})
AmNES/LIS-1	GPP[a]	7.57 ± 2.76	314.68 ± 12.90	0.021 ± 0.0008	2.75 ± 0.076
	FPP[b]	24.13 ± 1.23	1493.12 ± 41.33	0.099 ± 0.003	4.11 ± 0.19
	Mg^{2+} (GPP)[c]	1156 ± 62	265.18 ± 3.16	0.017 ± 0.002	0.015 ± 0.007
	Mg^{2+} (FPP)[d]	316 ± 2.9	1395.12 ± 18.12	0.092 ± 0.001	0.292 ± 0.006
AmNES/LIS-2	GPP[a]	7.68 ± 2.53	341.65 ± 8.21	0.022 ± 0.0005	2.94 ± 0.061
	FPP[b]	22.68 ± 0.66	1257.19 ± 26.75	0.083 ± 0.002	3.64 ± 0.03
	Mg^{2+} (GPP)[c]	1066 ± 16	294.58 ± 9.54	0.019 ± 0.0006	0.018 ± 0.003
	Mg^{2+} (FPP)[d]	339 ± 5.4	1247.32 ± 8.39	0.082 ± 0.005	0.243 ± 0.005

All values represent mean ± SE, n = 3. K_m, the Michaelis constant; V_{max}, the maximal velocity; K_{cat}, turnover number of enzyme.
[a]At 6 mM Mg^{2+}.
[b]At 8 mM Mg^{2+}.
[c]At 43 μM GPP.
[d]At 72 μM FPP.

post-translational controls also contribute to regulation in 10- to 12-day-old flowers. High levels of TPS activities in mature and old flowers (day 7–12 postanthesis), with low to no concomitant emission of volatile products, indicate that the levels of available substrates in the cell are also involved in the regulation of the biosynthesis and emission of linalool and nerolidol.

Discussion

Two bifunctional nerolidol/linalool synthases are involved in linalool and nerolidol biosynthesis in snapdragon flowers

Linalool and nerolidol formation in plant cells could either require two specialized TPSs, linalool and nerolidol syn-

Figure 6. Confocal laser scanning microscopy of transiently expressed AmNES/LIS-GFP fusions in Arabidopsis protoplasts.
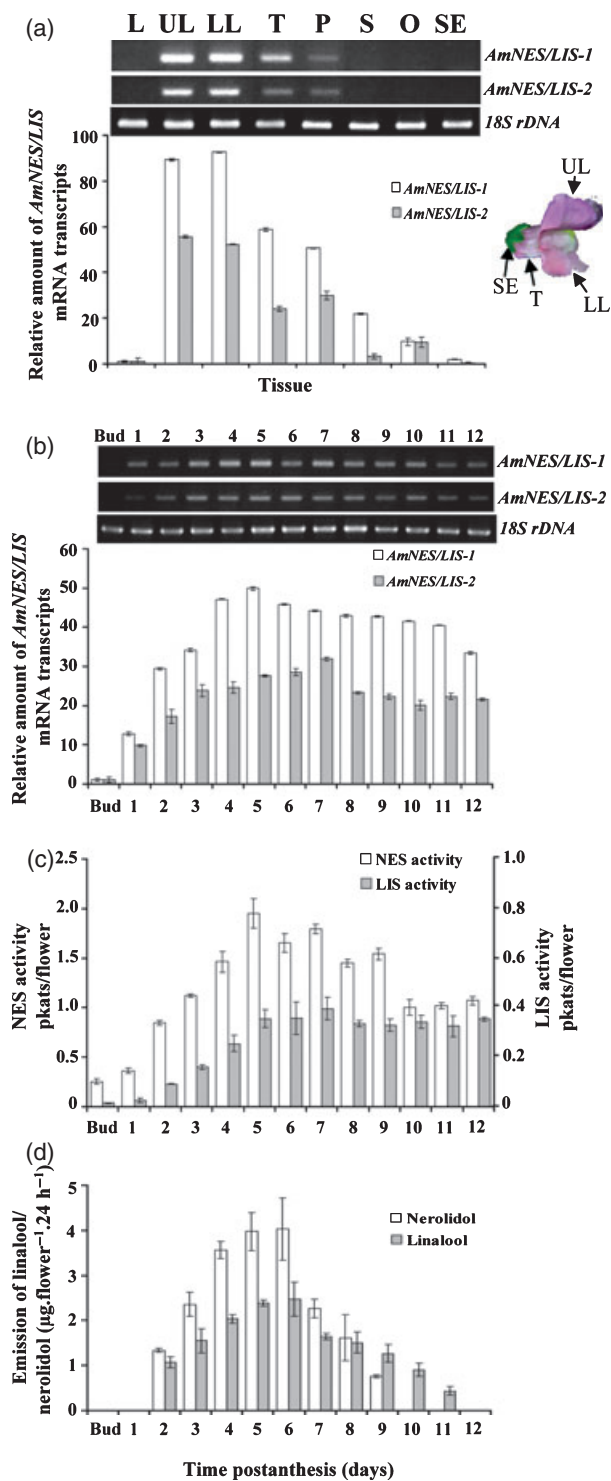GFP fusion constructs are shown on the left, and the corresponding transient expression in the protoplast is shown on the right; TP, transit peptide. Green fluorescent protein fluorescence detected in the green channel is shown in the 'Green' column; chlorophyll autofluorescence detected in the red channel is shown in the 'Red' column; the 'Merged' column shows combined red and green channels; the 'Transmission' column shows light-microscopy images of intact protoplasts. The results of two independent experiments are shown for each fusion construct, except for the controls (GFP and RbTP-GFP). RbTP (plastidial RuBisCO target peptide)-GFP is a chloroplast marker. Scale bars: 50 μm. The numbers in the fusion constructs correspond to amino acid positions.
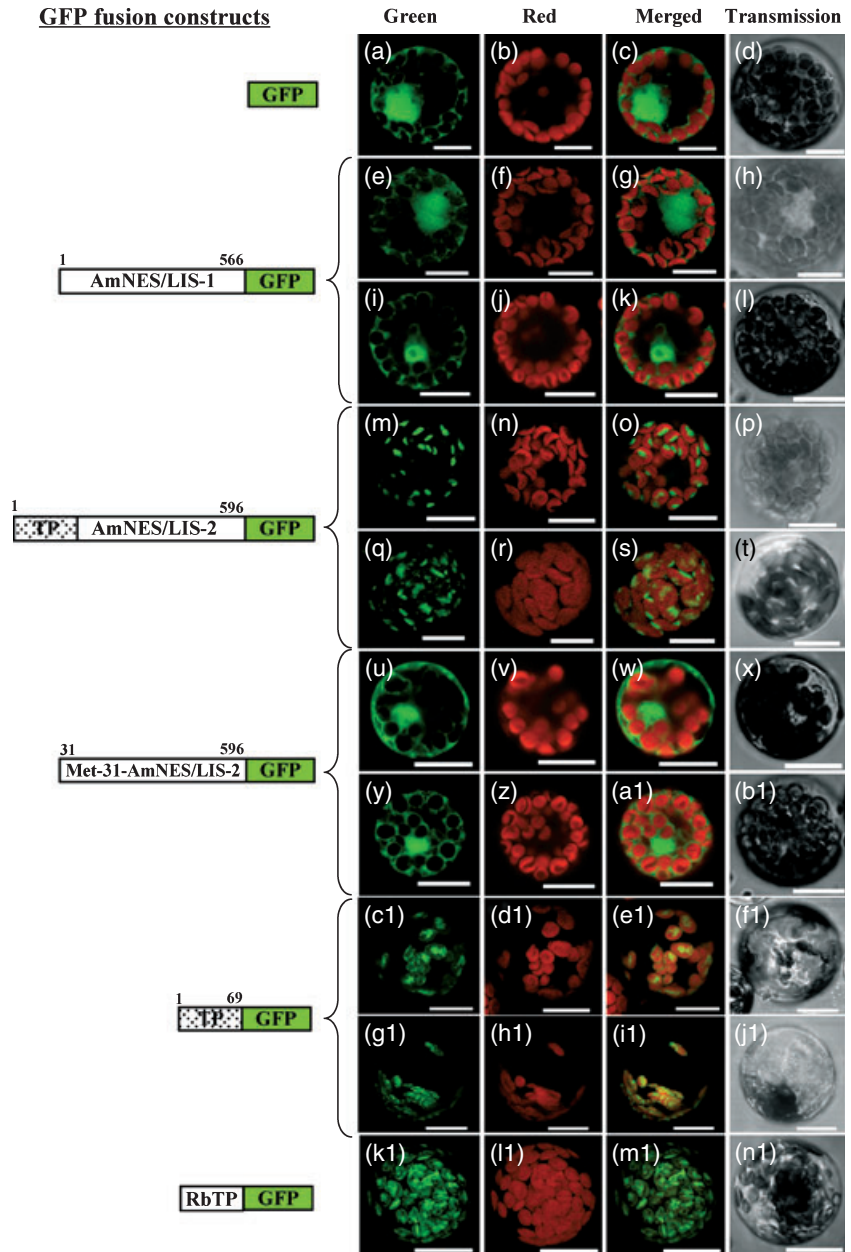
thase, or be the result of a bifunctional nerolidol/linalool synthase. Linalool synthases have been isolated and functionally characterized from a wide range of plant species, including the angiosperms *Clarkia breweri* (Pichersky *et al.*, 1995), *Artemisia annua* (Jia *et al.*, 1999), *Mentha citrata* (Crowell *et al.*, 2002), *Arabidopsis thaliana* (Chen *et al.*, 2003), *Lycopersicon esculentum* (van Schie *et al.*, 2007) and the gymnosperm *Picea abies* (Martin *et al.*, 2004). These linalool synthases produce linalool as the sole or predominant product from GPP, and possess an N-terminal transit peptide that directs their import into plastids. Four linalool synthases were examined for their ability to use FPP as a substrate. In contrast to *Artemisia* and *Clarkia* linalool syn-

thases, which were inactive with FPP (Aharoni *et al.*, 2004; Jia *et al.*, 1999), Arabidopsis and tomato linalool synthases were able to convert FPP to nerolidol, which was not found in their tissues. Whereas in Arabidopsis nerolidol formation occurred at a rate that was 50-fold lower than the rate of formation of linalool from GPP (Chen *et al.*, 2003), no information about the efficiency of nerolidol biosynthesis relative to linalool formation was provided in tomato (van Schie *et al.*, 2007).

Enzymes reported to be bona fide nerolidol synthases have only been characterized from maize and strawberry. (*E*)-Nerolidol was the only product formed from FPP *in vitro* by strawberry FaNES enzymes (*Fragaria ananassa* nerolidol

Figure 7. *AmNES/LIS* mRNA expression, linalool and nerolidol synthase activities, and emission of corresponding compounds in snapdragon flowers. Semiquantitative (gels) and quantitative RT-PCR (graph) analysis of *AmNES/LIS-1* and *AmNES/LIS-2* expression in different floral tissues of 5-day-old snapdragon flowers (a) and petal lobes during flower development from mature buds from 1 day before opening to 12 days postanthesis (b). Abbreviations: L, young leaves; UL and LL, upper and lower petal lobes, respectively; T, tubes; P, pistils; S, stamens; O, ovaries; SE, sepals. *AmNES/LIS-1* and *AmNES/LIS-2* mRNA expression in leaves (a) and buds (b) was set to 1 to determine the relative abundances of mRNA transcripts. Each point is an average of between three and five independent experiments. Vertical bars indicate standard error values. 18S rDNA was used as an endogenous reference in semiquantitative and quantitative RT-PCR.
(c) Changes in linalool and nerolidol synthase activities in snapdragon petal lobes during flower development. For each point, enzyme assays were run in duplicate on two independent crude extracts and standard deviations were obtained.
(d) Nerolidol and linalool emission from snapdragon flowers. Headspace collections were performed at 24-h intervals. Each point represents an average of between three and five independent experiments. Vertical bars indicate standard deviations.

2004), and with TPS1 being four times less active with GPP than with FPP (Schnee *et al.*, 2002).

To discover genes responsible for scent production in snapdragon flowers, and to understand the molecular mechanisms that control volatile emission, we have identified and characterized two nearly identical (95% aa identity) nerolidol/linalool synthases, AmNES/LIS-1 and AmNES/LIS-2, which were the two remaining uncharacterized enzymes responsible for the terpenoid profile of snapdragon scent. These enzymes share ∼50% identity with FaNES proteins, and, similar to FaNES, catalyze the formation of linalool or nerolidol, depending on the type of precursor used (GPP for monoterpenes and FPP for sesquiterpenes; Figure 3).

The recombinant AmNES/LIS proteins produced in *E. coli* exhibit very similar catalytic efficiency towards GPP and FPP, although with a slight preference for FPP (Table 1). The apparent K_m value of snapdragon nerolidol/linalool synthases for GPP is three times lower than that for FPP (∼7.6 versus ∼24 μM for GPP and FPP, respectively; Table 1), in contrast to FaNES1, which has an apparent K_m for GPP that is 3.6 times higher than that for FPP (29.0 versus 8.1 μM for GPP and FPP, respectively; Aharoni *et al.*, 2004). Although the apparent K_m values of the AmNES/LIS enzymes for GPP and FPP are relatively high, when compared with those of monoterpene synthases for GPP (the low μM range) and sesquiterpene synthases for FPP (0.1–10 μM), the turnover rates (k_{cat}) with both substrates are within the range reported for monoterpene (0.01–1.0 sec^{-1}) and sesquiterpene (0.03–0.5 sec^{-1}) synthases (Cane, 1999; Wise and Croteau, 1999). Moreover, apparent K_m values of AmNES/LIS enzymes for GPP were lower than those reported for linalool synthases from *M. citrata* (56 μM; Crowell *et al.*, 2002) and *A. annua* (64 μM; Jia *et al.*, 1999). The ability of TPSs to accept both GPP and FPP is not unique to linalool/nerolidol synthases, and has been well documented in sesquiterpene synthases from *Mentha piperita* (Crock *et al.*, 1997), *Malus domestica*

synthase; Aharoni *et al.*, 2004). Maize TPS1 produced nerolidol as one of the products (29% of total product), in addition to (*E*)-β-farnesene (26%) and (*E,E*)-farnesol (45%; Schnee *et al.*, 2002). Both enzymes were able to catalyze linalool formation from GPP *in vitro*, with FaNES forming both linalool and nerolidol with equal efficiency (Aharoni *et al.*,

(Green *et al.*, 2007; Pechous and Whitaker, 2004), *Abies grandis* (Bohlmann *et al.*, 1998a; Steele *et al.*, 1998), *L. esculentum* (Colby *et al.*, 1998), *A. annua* L (Mercke *et al.*, 1999), *A. thaliana* (Tholl *et al.*, 2005), *O. basilicum* (Iijima *et al.*, 2004) and *Zea mays* (Kollner *et al.*, 2004). However, their sesquiterpene synthase activities significantly exceeded their monoterpene synthase activities.

Linalool and nerolidol biosynthesis in snapdragon is compartmentally segregated

It is generally accepted that monoterpene biosynthesis takes place in plastids, where GPP is synthesized, whereas sesquiterpene formation occurs in the cytosol, where FPP is formed (Aharoni *et al.*, 2005). Thus, compartmental separation of precursors for monoterpene and sesquiterpene biosynthesis would prevent a bifunctional monoterpene/sesquiterpene synthase from using both of its activities, unless it is localized in both compartments. However, recent metabolic engineering in Arabidopsis, tobacco and potato revealed the existence of small levels of FPP in plastids and GPP in the cytosol (Aharoni *et al.*, 2003, 2006; Wu *et al.*, 2006). The presence of substrate for monoterpene and sesquiterpene biosynthesis in both plastids and cytosol, although at different levels (high GPP/trace FPP in plastid and vice versa in cytosol), would allow a dual functional enzyme to produce monoterpenes and sesquiterpenes in both compartments, but at a ratio representative of that of the precursors. Indeed, overexpression of strawberry *FaNES1* in plastids of Arabidopsis and potato resulted in the formation of small quantities of nerolidol, which was 100- to 300-fold lower than the quantity of linalool that was produced (Aharoni *et al.*, 2003, 2006).

Here, we show that snapdragon flowers emit linalool and nerolidol, the levels of which are developmentally regulated, and are of a similar order of magnitude (Figure 7d). These compounds are synthesized by two nearly identical AmNES/LIS proteins that exhibit different subcellular localization. AmNES/LIS-1 is localized in the cytosol and is responsible for nerolidol biosynthesis, whereas AmNES/LIS-2 has a transit peptide directing it to plastids, and accounts for linalool formation (Figure 6). Nerolidol formation from FPP and linalool from GPP by purified leucoplasts also confirmed the presence of both monoterpene/sesquiterpene synthase activities in plastids (Figure 5e,f). The coexistence of AmNES/LIS-1 and AmNES/LIS-2 enzymes with dual monoterpene/sesquiterpene activities in the cytoplasm and leucoplasts does not exclude the possibility that minute quantities of linalool and nerolidol can be synthesized in the cytosol and plastids, respectively, as a result of the possible trace levels of GPP and FPP derived from promiscuous side reactions of FPP and GGPP synthases in the corresponding cellular compartments. However, exogenously supplied $[^2H_2]$mevalolactone ($[^2H_2]$MVL), to cut snapdragon flowers efficiently, labeled nerolidol and showed no detectable incorporation in linalool (Dudareva *et al.*, 2005), suggesting that if a GPP pool exists in the cytosol, it is small and does not contribute significantly to linalool formation. Moreover, snapdragon GPP synthase was localized in plastids, indicating that GPP biosynthesis takes place predominantly in leucoplasts (Tholl *et al.*, 2004); there is no direct evidence for plastidial FPP synthase.

Although linalool and nerolidol are components of snapdragon floral scent, they are also major volatiles of fruit flavor in ripe strawberry (Aharoni *et al.*, 2004). Similar to snapdragon, the cultivated strawberry genome contains two genes, *FaNES1* and *FaNES2*, each encoding an enzyme with dual linalool/nerolidol synthase activities *in vitro*. It has been shown that FaNES1 and FaNES2 are localized in the cytosol and plastids, respectively. Although the *FaNES1* gene was highly expressed in ripe strawberry fruits, *FaNES2* expression was barely detectable. Based on these results, Aharoni *et al.* (2004) concluded that both linalool and nerolidol are formed by FaNES1 in the cytosol, and that strawberry cytoplasm contains sufficient levels of GPP and FPP for the biosynthesis of roughly similar quantities of linalool and nerolidol, although the pools of available substrates in fruit tissue are not known (Aharoni *et al.*, 2004). Moreover, this work did not disprove plastidial formation of linalool, as linalool synthase activity was not checked in purified plastids isolated from strawberry fruits, and nor were any genetic or proteomic proofs provided.

Recently, Hampel *et al.* (2006) suggested that strawberry fruits synthesize terpenoids exclusively via the cytosolic MVA pathway, based on $[^2H_2]$MVL incorporation and a lack of labeling with deuterium-labeled 1-deoxy-[5,5-$^2H_2$]-D-xylulose ($[^2H_2]$DOX), in contrast to snapdragon flowers, where both plastidial monoterpene and cytosolic sesquiterpene biosyntheses rely on MEP pathway derived precursors (Dudareva *et al.*, 2005). Although the MVA pathway is localized in the cytosol, the results obtained in fruits do not exclude the possible transport of IPP formed from labeled MVL to plastids for linalool biosynthesis. The absence of detectable $[^2H_2]$DOX labeling of terpenoids in fruit tissue could result from a lack of D-xylulose kinase, which catalyzes the phosphorylation of exogenously supplied DOX (Hemmerlin *et al.*, 2006) in order for it to enter the pathway and be utilized. Unfortunately, D-xylulose kinase activity was not checked in fruit tissue, leaving the actual contributions of the MEP pathway to terpenoid biosynthesis in strawberry fruits yet to be determined.

Similar to snapdragon, nearly identical but compartmentally separated enzymes exist in monocotyledons. Maize plants contain TPS1, which is capable of producing (*E*)-nerolidol, (*E*)-β-farnesene and (*E,E*)-farnesol from FPP, and linalool from GPP *in vitro* (Schnee *et al.*, 2002). Attack on maize cv. B73 by Egyptian cotton leafworms (*Spodoptera littoralis*) increases *tps1* transcript levels by around eightfold

over the basal level, and induces emission of (*E*)-β-farnesene, linalool and a metabolite of (*E*)-nerolidol, (*3E*)-4,8-dimethyl-1,3,7-nonatriene (DMNT). Although Schnee *et al.* (2002) reported TPS1 to be localized in the cytosol and to be responsible for sesquiterpene formation, our computer analysis of its subcellular localization using five search algorithms predicted its plastidial location, suggesting it could be involved in linalool formation. In order for TPS1 to catalyze (*E*)-nerolidol and (*E*)-β-farnesene formation, similar enzyme(s) must exist in the cytosol. Indeed, genes encoding proteins closely related to TPS1 have recently been identified in maize, and may be localized in the cytosol (J. Degenhardt and J. Gershenzon, personal communication).

Substrate availability in the cell determines the product type formed, and regulates developmental linalool/nerolidol emission in snapdragon

Linalool and nerolidol emission during flower development follows similar patterns to other terpenoids and phenyl-propanoids within the snapdragon scent bouquet (Dudareva *et al.*, 2000, 2003): peaking on day 5–6 postanthesis and declining thereafter (Figure 7d). Nerolidol and linalool synthase activities follow two different profiles, and belong to two different groups of scent biosynthetic enzymes based on developmental activity (Dudareva and Pichersky, 2000). Despite high levels of nerolidol/linalool synthase activities in old snapdragon flowers, emission of the corresponding compounds declines (Figure 7c,d), suggesting that substrate availability plays a role in the regulation of formation and emission of these compounds. Moreover, our previous labeling experiments showed that the exogenous supply of [^{2}H$_2$]MVL increased nerolidol emission by 2.4- and 10-fold during the day and night, respectively, suggesting that the capacity of AmNES/LIS-1 for nerolidol production has not been exceeded, even in mature snapdragon flowers (Dudareva *et al.*, 2005). In these flowers, both monoterpenes and the sesquiterpene nerolidol are synthesized from MEP pathway derived IPP/DMAPP (Dudareva *et al.*, 2005). However, exogenously supplied [^{2}H$_2$]DOX had no effect on their emission profiles, indicating that flux towards GPP and FPP is tightly regulated.

Overall, our results show that two nearly identical TPSs with similar catalytic properties are responsible for the formation of different terpenoid products in different subcellular compartments. The subcellular localization of these bifunctional enzymes and substrate availability determine the type and quantity of product formed. Since many TPSs accept more than one substrate (Tholl, 2006), the direction of nearly identical bifunctional enzymes to different cellular compartments allows plants to extend the range of available substrates, thus increasing the diversity of synthesized metabolites. However, there is no evidence for the production of high levels of monoterpenes in cytosol, which is most

likely the result of a very small pool of GPP in this cellular compartment.

Experimental procedures

Plant material and headspace analysis of floral volatiles

Snapdragon (*A. majus*) cv. Maryland True Pink (Ball Seed, http://www.ballseed.com) was grown in a greenhouse (Dudareva *et al.*, 2000). Emitted volatiles were collected every 24 h at 09:00 h by the closed-loop stripping method (Donath and Boland, 1995) and were then analyzed following the methods described by Dudareva *et al.* (2000) and Kolosova *et al.* (2001).

Chemicals and radiochemicals

[1-^{3}H]-Geranyl diphosphate (GPP; 3.7 kBq mol^{-1}) and [1-^{3}H]-farnesyl diphosphate (FPP; 3.7 kBq mol^{-1}) were purchased from American Radiolabeled Chemicals (http://www.arcincusa.com). Unlabeled GPP (1 mg ml^{-1}) and FPP (1 mg ml^{-1}) were purchased from Echelon Research Laboratories (http://www.echelon-inc.com). Terpenoid standards and reagents were purchased from Sigma-Aldrich (http://www.sigmaaldrich.com) unless otherwise noted.

Sequence analysis

Amino acid sequence alignments were generated using the CLUSTALX computer program (http://align.genome.jp). Sequence relatedness was analyzed using the neighbor-joining method, and an unrooted tree was visualized using TREEVIEW (http://taxonomy.zoology.gla.ac.uk/rod/treeview.html).

Expression of AmNES/LIS proteins in E. coli and purification of recombinant proteins

As both full-length AmNES/LIS cDNA clones from a snapdragon EST collection had an intron, the corresponding open reading frames were obtained by reverse transcriptase (RT) PCR amplification of RNA from 5-day-old snapdragon petal tissues. Forward primers were 5′-<u>CATATG</u>AGTAACCTTCATGTAAAG-3′ for AmNES/LIS-1 and 5′-<u>CATATGG</u>CATTTTATATTGGCAACAAC-3′ for AmNES/LIS-2, and introduced an *Nde*I site (underlined) at the initiating ATG codon. Reverse primers were 5′-<u>CTCGAG</u>ATCAAACAACTAAATCTTAACATAC-3′ for AmNES/LIS-1 and 5′-<u>CTCGAG</u>ATCAAACAACATAAACTTAACATAC-3′ for AmNES/LIS-2, and contained an *Xho*I site (underlined), which allowed a translational fusion to a C-terminal (His)$_6$-tag. Truncated versions of AmNES/LIS-2 were amplified from AmNES/LIS-2 cDNA by PCR using the AmNES/LIS-1 forward primer for Met-31-AmNES/LIS-2 and the 5′-CATATGGACTTGAATGGACAAAG-3′ forward primer for Met-79-AmNES/LIS-2, both in combination with the AmNES/LIS-2 reverse primer. The amplified coding regions were subcloned in-frame and upstream of the (His)$_6$-tag of the pET32a expression vector (Novagen, http://www.emd-biosciences.com). Sequencing revealed that no errors had been introduced.

For functional expression, *E. coli* BL21 Rosetta competent cells were transformed with recombinant plasmids and pET32a lacking an insert (control). Induction, harvesting and protein purification by affinity chromatography on nickel-nitrilotriacetic acid-agarose (Qiagen, http://www.qiagen.com) were performed as described by Negre *et al.* (2002) and Kaminaga *et al.* (2006). The purity of the

proteins was determined by densitometry of the SDS-PAGE gels after Coomassie Brilliant Blue staining, and ranged from 65% to 72%. The protein concentration was determined by the Bradford method (Bradford, 1976).

Terpene synthase assays and product identification

Assays for TPS activity were performed in a 100-μl assay buffer (30 mM HEPES, pH 7.5, 5 mM DTT, and 1 mM or 40 mM MgCl$_2$) containing recombinant protein (0.58–0.66 μg) or plant crude extract (50–100 μg of protein), and 41/72 μM [1-^{3}H]GPP/FPP (55 mCi m-mol^{-1}). The mixture was immediately overlaid with 1 ml of hexane. After a 15-min incubation at 30°C, reaction products (and alcohols produced by endogenous phosphohydrolase activity) were extracted into the hexane phase and a volume of 600 μl was counted (Boatright *et al.*, 2004). Extracts from *E. coli* transformed with pET-32a lacking an insert and heat-denatured enzymes served as controls.

For identification of reaction products, large-scale assays (1000 μl) were performed using purified AmNES/LIS proteins, crude extracts from flowers, and purified leucoplasts from petals using unlabeled FPP and GPP (60 μM) with the solid-phase microextraction (SPME) system. After incubation for 1 h at 30°C and 15 min at 42°C, synthesized volatiles were analyzed by GC-MS. Chiral GC-MS analysis was performed on the same instrument equipped with 2,3-di-*O*-methyl-6-*O*-*tert*-butyl dimethylsilyl beta cyclodextrin doped into a 14% cyanopropylphenyl/86% dimethyl polysiloxane (Rt^{TM}-βDEXsm) column (30-m × 0.25-mm inner diameter; Restek, http://www.restek.com) under conditions specified by the manufacturer.

For detecting linalool synthase activity, the total monoterpene synthase activity determined using radiolabeled GPP was split amongst three monoterpene compounds, myrcene, (*E*)-β-ocimene, and linalool, based on the level of products produced by the same crude extracts from unlabeled GPP as determined by SPME.

Purification of native AmNES/LIS proteins from snapdragon petals

Protein purification was performed as described in Murfitt *et al.* (2000), except for the extraction buffer that contained 30 mM HEPES, pH 8.0, 1 mM DTT, 1 mM phenylmethanesulfonyl fluoride and 10% (v/v) glycerol (buffer A) with 1% (w/v) polyvinylpyrrolidone (PVP-40). After (DEAE)–cellulose (Whatman, http://www.whatman.com) column chromatography, fractions with the highest monoterpene and sesquiterpene synthase activities in the 230–280 mM KCl range were loaded on a HiTrap-Q FF column (Pharmacia Biotech Inc.) pre-equilibrated with buffer A. TPSs were eluted with the linear gradient of 0–1 M KCl, and fractions with the highest monoterpene and ses-quiterpene synthase activities were subjected to size-exclusion gel filtration chromatography on a HiLoad^{TM} 16/60 Superdex^{TM} 200 column (Pharmacia Biotech Inc.), which resulted in three 1-ml active fractions. These fractions were precipitated with trichloroacetic acid (20% final concentration; Kohlstaedt, 2006), and were examined by SDS-PAGE followed by gel staining with Coomassie brilliant blue.

Protein sequencing

The ∼60-kDa protein band from the combined size-exclusion fractions with the highest TPS activities as well as surrounding proteins within 1 cm were excised from the SDS-PAGE gel, digested with trypsin and sequenced by LC-MS/MS as described by Chen *et al.*

(2005), followed by the screening of a snapdragon EST database comprising more than 25 000 sequences using the MASCOT program (Perkins *et al.*, 1999). Five unique peptides obtained from the protein band (SKREEEPIDR, LMFVDAIQR, FRGELQR, GLMELYEASQLR and LQHPYR) matched predicted protein sequences of both AmNES/LIS-1 and AmNES/LIS-2 with a significance threshold of 0.05. A sixth peptide (LGVNHNFEELIETILR) matched only AmNES/LIS-1. Eight peptides (HLLHLK, LGVNHHFQK, EIEEILRK, YVSA-DVFNNFK, FKEELKR, NYDDDLGGMYEWGK, ESFNLNHDSVSSFK and GPVLEEYVK) matched protein sequences of previously char-acterized myrcene and ocimene synthases (Dudareva *et al.*, 2003), whereas six peptides (GENDPIESLIFVDATLR, YPFHTSIAR, HGYN-PIDSLK, GSIELNDTQELMSSIAIIFR, QAALNLAR and MVPLMY-SYDHNQR) matched only myrcene synthase. At this stringency, no peptide hits to other TPSs in the EST database were found.

Determination of AmNES/LIS kinetic properties

For kinetic analysis, an appropriate enzyme concentration was chosen so that the reaction velocity was proportional to the enzyme concentration, and was linear with respect to incubation. Kinetic data were evaluated using Lineweaver–Burk, Eadie–Hofstee and Hanes plots.

RNA isolation and real-time RT-PCR

Total RNA from leaves and floral tissues was isolated and analyzed as described previously (Dudareva *et al.*, 1996, 1998, 2000; Kolosova *et al.*, 2001). One microgram of total RNA was used to prepare cDNA according to the manufacturer's instructions (High-Capacity cDNA Archive Kit; Applied Biosystems, http://www.appliedbiosys-tems.com). A linear range of cDNA was used for real-time PCR. Real-time quantitative reverse transcriptase polymerase chain reaction (real-time RT-PCR) was performed in a 96-well plate using a Gene-Amp 5700 sequence detection system (PE Applied Biosystems, Foster City, CA, USA) with SYBR green fluorescent dye. A 250-bp fragment in the 3′ region of the coding sequence was amplified using gene-specific primers: forward 5′-AAAGAACATATAAGCT-TGTCGAC-3′ and reverse 5′-GTTCTTTAATTGGTAGTGCTTCG-3′ for AmNES/LIS-1, forward 5′-AAAGAACATACAAGCTTGTCGCT-3′ and reverse 5′-GTTCTTTAATTGGTAGTGCTCGA-3′ for AmNES/LIS-2, forward 5′-TGGTCGCAAGGCTGAAACTTAAAGGA-3′ and reverse 5′-ACCAGACAAATCGCTCCACCAACTAA-3′ for 18S cDNA. Real-time RT-PCRs were performed in a 20-μl reaction mixture containing forward and reverse primers according to the manufacturer's pro-tocol (PE Applied Biosystems). Real-time RT-PCR conditions were as follows: 94°C for 10 min for one cycle, followed by 40 cycles of 94°C for 15 sec, 54°C for 15 sec and 72°C for 15 sec. Several real-time RT-PCRs were run per sample in triplicate per run. The quan-tification of gene expression was performed using the comparative cycle threshold (C_t) method (Applied Biosystems).

Subcellular localization of AmNES/LIS proteins

The open reading frames of AmNES/LIS-1, AmNES/LIS-2, Met-31-AmNES/LIS-2 and the first 69 aa of AmNES/LIS-2 were fused up-stream of, and in frame with, GFP in the cloning sites *Xba*I and *Bam*HI of the p326-SGFP vector containing the CaMV 35S promoter (a gift from Dr I. Hwang Pohang, University of Science and Tech-nology, Korea). Sequencing confirmed the accuracy of the fusion. *Arabidopsis* protoplasts were transformed as described by Sheen (2002). DNA from each construct (20 μg) was used for PEG-mediated

transformation of 100 μl of ice-cold protoplasts. p326-SGFP and p326-RbTP-SGFP were markers for cytosolic and plastidial localization. Transient expression of GFP fusion proteins was observed 16–20 h after transformation using MRC-1024 UV (Bio-Rad, http://www.bio-rad.com) on a Diaphot 300 (Nikon, http://www.nikon.com) inverted microscope with a 60 × 1.4 numerical aperture lens. The 488-nm line of the krypton–argon laser (Ion Laser Technology; http://www.medizin.li) was used to excite GFP. Fluorescence was collected with a 522/35 bandpass filter. Chlorophyll fluorescence was excited using the 568-nm line of the krypton–argon laser, and emission was collected with a 680DF32 filter.

Leucoplast isolation

Leucoplasts were isolated according to the method described by Kang and Rawsthorne (1994), and were purified using a discontinuous Percoll gradient (Smith *et al.*, 1992). The gradient consisted of 2 ml 70% Percoll, 4 ml of each of 50, 35, 22 and 10% PBF-Percoll, and leucoplasts were collected from the 22–35% interface after 8 min of centrifugation at 9200 ***g*** using a Sorvall HB-6 swing-out rotor. The integrity of the resulting leucoplasts was confirmed by scanning electron microscopy, and yield and cytosolic contamination were assessed by measuring NADP-glyceraldehyde-3-phosphate dehydrogenase and alcohol dehydrogenase activities (Kang and Rawsthorne, 1994). No alcohol dehydrogenase activity was detected in purified plastids.

Statistical analysis

The correlation between TPS activities and the emission of corresponding terpenoid compounds was analyzed by ANOVA using the JMP statistical package (version 6.0.2; http://www.jmp.com).

Acknowledgements

Supplementary Material

The following supplementary material is available for this article online:
Figure S1. Purification of AmNES/LIS from snapdragon flowers.
Figure S2. Activities of marker enzymes in total crude extract and leucoplast fractions of snapdragon petal tissue.
This material is available as part of the online article from http://www.blackwell-synergy.com.
Please note: Blackwell Publishing are not responsible for the content or functionality of any supplementary materials supplied by the authors. Any queries (other than missing material) should be directed to the corresponding author for the article.

References

Aharoni, A., Giri, A.P., Deuerlein, S., Griepink, F., de Kogel, W.J., Verstappen, F.W., Verhoeven, H.A., Jongsma, M.A., Schwab, W. and Bouwmeester, H.J. (2003) Terpenoid metabolism in wild-type and transgenic Arabidopsis plants. *Plant Cell*, **15**, 2866–2884.

Aharoni, A., Giri, A.P., Verstappen, F.W., Bertea, C.M., Sevenier, R., Sun, Z., Jongsma, M.A., Schwab, W. and Bouwmeester, H.J. (2004) Gain and loss of fruit flavor compounds produced by wild and cultivated strawberry species. *Plant Cell*, **16**, 3110–3131.

Aharoni, A., Jongsma, M.A. and Bouwmeester, H.J. (2005) Volatile science? Metabolic engineering of terpenoids in plants *Trends Plant Sci.* **10**, 594–602.

Aharoni, A., Jongsma, M.A., Kim, T.Y., Ri, M.B., Giri, A.P., Verstappen, W.A., Schwab, W. and Bouwmeester, H.J. (2006) Metabolic engineering of terpenoid biosynthesis in plants. *Phytochem. Rev.* **5**, 49–58.

Aubourg, S., Lecharny, A. and Bohlmann, J. (2002) Genomic analysis of the terpenoid synthase (AtTPS) gene family of *Arabidopsis thaliana. Mol. Genet. Genomics*, **267**, 730–745.

Bey, M., Stuber, K., Fellenberg, K., Schwarz-Sommer, Z., Sommer, H., Saedler, H. and Zachgo, S. (2004) Characterization of Antirrhinum petal development and identification of target genes of the class B MADS box gene *DEFICIENS. Plant Cell*, **16**, 3197–3215.

Boatright, J., Negre, F., Chen, X., Kish, C.M., Wood, B., Peel, G., Orlova, I., Gang, D., Rhodes, D. and Dudareva, N. (2004) Understanding *in vivo* benzenoid metabolism in petunia petal tissue. *Plant Physiol.* **135**, 1993–2011.

Bohlmann, J., Crock, J., Jetter, R. and Croteau, R.B. (1998a) Terpenoid-based defenses in conifers: cDNA cloning, characterization, and functional expression of wound-inducible (*E*)-alpha-bisabolene synthase from grand fir (*Abies grandis*). *Proc. Natl Acad. Sci. USA*, **95**, 6756–6761.

Bohlmann, J., Meyer–Gauen, G. and Croteau, R. (1998b) Plant terpenoid synthases: molecular biology and phylogenetic analysis. *Proc. Natl Acad. Sci. USA*, **95**, 4126–4133.

Bradford, M.M. (1976) A rapid and sensitive method for the quantitation of microgram quantities of protein utilizing the principle of protein-dye binding. *Anal. Biochem.* **72**, 248–254.

Cane, D.E. (1999) Sesquiterpene biosynthesis: cyclization mechanisms. In *Comprehensive Natural Products Chemistry, Vol. 2, Isoprenoids Including Carotenoids and Steroids* (Cane, D.D., ed.). Amsterdam: Elsevier, pp. 155–200.

Chen, F., Tholl, D., D'auria, J.C., Farooq, A., Pichersky, E. and Gershenzon, J. (2003) Biosynthesis and emission of terpenoid volatiles from Arabidopsis flowers. *Plant Cell*, **15**, 1–15.

Chen, H., Wilkerson, C.G., Kuchar, J.A., Phinney, B.S. and Howe, G.A. (2005) Jasmonate-inducible plant enzymes degrade essential amino acids in the herbivore midgut. *Proc. Natl Acad. Sci. USA*, **102**, 19237–19242.

Colby, S.M., Crock, J., Dowdle–Rizzo, B., Lemaux, P.G. and Croteau, R. (1998) Germacrene C synthase from *Lycopersicon esculentum* cv. VFNT cherry tomato: cDNA isolation, characterization, and bacterial expression of the multiple product sesquiterpene cyclase. *Proc. Natl Acad. Sci. USA*, **95**, 2216–2221.

Crock, J., Wildung, M. and Croteau, R. (1997) Isolation and bacterial expression of a sesquiterpene synthase cDNA clone from peppermint (*Mentha* × *piperita*, L.) that produces the aphid alarm pheromone (*E*)–β–farnesene. *Proc. Natl Acad. Sci. USA*, **94**, 12833–12838.

Crowell, A.L., Williams, D.C., Davis, E.M., Wildung, M.R. and Croteau, R. (2002) Molecular cloning and characterization of a new linalool synthase. *Arch. Biochem. Biophys.* **405**, 112–121.

Donath, J. and Boland, W. (1995) Biosynthesis of acyclic homoterpenes – enzyme selectivity and absolute configuration of the nerolidol precursor. *Phytochemistry*, **39**, 785–790.

Dudareva, N. and Pichersky, E. (2000) Biochemical and molecular genetic aspects of floral scents. *Plant Physiol.* **122**, 627–633.

Dudareva, N., Cseke, L., Blanc, V.M. and Pichersky, E. (1996) Evolution of floral scent in *Clarkia*: novel patterns of *S*-linalool synthase gene expression in the *C. breweri* flower. *Plant Cell*, **8**, 1137–1148.

Dudareva, N., D'Auria, J.C., Nam, K.H., Raguso, R.A. and Pichersky, E. (1998) Acetyl-CoA:benzyl alcohol acetyltransferase: an enzyme involved in floral scent production in *Clarkia breweri*. *Plant J.* **14**, 297–304.

Dudareva, N., Murfitt, L.M., Mann, C.J., Gorenstein, N., Kolosova, N., Kish, C.M., Bonham, C. and Wood, K. (2000) Developmental regulation of methylbenzoate biosynthesis and emission in snapdragon flowers. *Plant Cell*, **12**, 949–961.

Dudareva, N., Martin, D., Kish, C.M., Kolosova, N., Gorenstein, N., Fäldt, J., Miller, B. and Bohlmann, J. (2003) (*E*)-β-ocimene and myrcene synthase genes of floral scent biosynthesis in snapdragon: function and expression of three terpene synthase genes of a new terpene synthase subfamily. *Plant Cell*, **15**, 1227–1241.

Dudareva, N., Andersson, S., Orlova, I., Gatto, N., Reichelt, M., Rhodes, D., Boland, W. and Gershenzon, J. (2005) The nonmevalonate pathway supports both monoterpene and sesquiterpene formation in snapdragon flowers. *Proc. Natl Acad. Sci. USA*, **102**, 933–938.

Dudareva, N., Negre, F., Nagegowda, D.A. and Orlova, I. (2006) Plant volatiles: recent advances and future perspectives. *Crit. Rev. Plant Sci.* **25**, 417–440.

Gershenzon, J. and Kreis, W. (1999) Biochemistry of terpenoids: monoterpenes, sesquiterpenes, diterpenes, sterols, cardiac glycosides and steroid saponins. In *Biochemistry of Plant Secondary Metabolism* (Wink, M., ed.). Boca Raton, FL: CRC Press, pp. 222–299.

Green, S., Friel, E.N., Matich, A., Beuning, L.L., Cooney, J.M., Rowan, D.D. and Macrae, E. (2007) Unusual features of a recombinant apple alpha-farnesene synthase. *Phytochemistry*, **68**, 176–188.

Hampel, D., Mosandl, A. and Wust, M. (2006) Biosynthesis of mono- and sesquiterpenes in strawberry fruits and foliage: ^{2}H labeling studies. *J. Agric. Food. Chem.* **54**, 1473–1478.

Hemmerlin, A., Hoeffer, J.F., Meyer, O., Tritsch, D., Kagan, I.A., Grosdemange-Billiard, C., Rohmer, M. and Bach, T.J. (2003) Cross-talk between the cytosolic mevalonate and the plastidal methylerythrito phosphate pathways in tobacco bright yellow-2 cells. *J. Biol. Chem.* **278**, 26666–26676.

Hemmerlin, A., Tritsch, D., Hartmann, M., Pacaud, K., Hoeffler, J.F., van Dorsselaer, A., Rohmer, M. and Bach, T.J. (2006) A cytosolic Arabidopsis D-xylulose kinase catalyzes the phosphorylation of 1-deoxy-D-xylulose into a precursor of the plastidial isoprenoid pathway. *Plant Physiol.* **142**, 441–457.

Iijima, Y., Davidovich-Rikanati, R., Fridman, E., Gang, D.R., Bar, E., Lewinsohn, E. and Pichersky, E. (2004) The biochemical and molecular basis for the divergent patterns in the biosynthesis of terpenes and phenylpropenes in the peltate glands of three cultivars of basil. *Plant Physiol.* **136**, 3724–3736.

Jia, J.W., Crock, J., Lu, S., Croteau, R. and Chen, X.Y. (1999) (*3R*)-Linalool synthase from *Artemisia annua* L.: cDNA isolation, characterization, and wound induction. *Arch. Biochem. Biophys.* **372**, 143–149.

Kaminaga, Y., Schnepp, J., Peel, G. *et al.* (2006) Plant phenylacetaldehyde synthase is a bifunctional homotetrameric enzyme that catalyzes phenylalanine decarboxylation and oxidation. *J. Biol. Chem.* **281**, 23357–23366.

Kang, F. and Rawsthorne, S. (1994) Starch and fatty acid synthesis in plastids from developing embryos of oilseed rape. *Plant J.* **6**, 795–805.

Knudsen, J.T. and Gershenzon, J. (2006) The chemical diversity of floral scent. In *Biology of Floral Scent* (Dudareva, N. and Pichersky, E., eds). Boca Raton [u.a.]: Taylor & Francis, pp. 27–52.

Kohlstaedt, L. (2006) TCA precipitation of proteins. Available at: http://biology.berkeley.edu/crl/mass_spec/TCA_precipitation_of_proteins.pdf.

Kollner, T.G., Schnee, C., Gershenzon, J. and Degenhardt, J. (2004) The variability of sesquiterpenes cultivars is controlled by allelic emitted from two *Zea mays* variation of two terpene synthase genes encoding stereoselective multiple product enzymes. *Plant Cell*, **16**, 1115–1131.

Kolosova, N., Gorenstein, N., Kish, C.M. and Dudareva, N. (2001) Regulation of circadian methyl benzoate emission in diurnally and nocturnally emitting plants. *Plant Cell*, **13**, 2333–2347.

Koyama, T. and Ogura, K. (1999) Isopentenyl diphosphate isomerase and prenyltransferases. In *Comprehensive Natural Product Chemistry, Vol. 2* (Barton, D. and Nakanishi, K., eds). Oxford: Elsevier Science Ltd, pp. 69–96.

Laule, O., Furholz, A., Chang, H.S., Zhu, T., Wang, X., Heifetz, P.B., Gruissem, W. and Lange, M. (2003) Crosstalk between cytosolic and plastidial pathways of isoprenoid biosynthesis in *Arabidopsis thaliana*. *Proc. Natl Acad. Sci. USA*, **100**, 6866–6871.

Lichtenthaler, H.K. (1999) The 1-deoxy-D-xylulose-5-phosphate pathway of isoprenoid biosynthesis in plants. *Annu. Rev. Plant Physiol. Plant Mol. Biol.* **50**, 47–65.

Martin, D.M., Fäldt, J. and Bohlmann, J. (2004) Functional characterization of nine Norway spruce TPS genes and evolution of gymnosperm terpene synthases of the TPS-d subfamily. *Plant Physiol.* **135**, 1908–1927.

McCaskill, D. and Croteau, R. (1995) Monoterpene and sesquiterpene biosynthesis in glandular trichomes of peppermint (*Mentha x piperita*) rely exclusively on plastid-derived isopentenyl diphosphate. *Planta*, **197**, 49–56.

McGarvey, D.J. and Croteau, R. (1995) Terpenoid metabolism. *Plant Cell*, **7**, 1015–1026.

Mercke, P., Crock, J., Croteau, R.B. and Brodelius, P.E. (1999) Cloning, expression, and characterization of *epi*-cedrol synthase, a sesquiterpene cyclase from *Artemisia annua* L. *Arch. Biochem. Biophys.* **369**, 213–222.

Murfitt, L.M., Kolosova, N., Mann, C.J. and Dudareva, N. (2000) Purification and characterization of *S*-adenosyl-L-methionine:benzoic acid carboxyl methyltransferase, the enzyme responsible for biosynthesis of the volatile ester methyl benzoate in flowers of *Antirrhinum majus*. *Arch. Biochem. Biophys.* **382**, 145–151.

Negre, F., Kolosova, N., Knoll, J., Kish, C.M. and Dudareva, N. (2002) Novel *S*-adenosyl-L-methionine:salicylic acid carboxyl methyltransferase, an enzyme responsible for biosynthesis of methylsalicylate and methylbenzoate, is not involved in floral scent production in snapdragon flowers. *Arch. Biochem. Biophys.* **406**, 261–270.

Newman, J.D. and Chappell, J. (1999) Isoprenoid biosynthesis in plants: carbon partitioning within the cytoplasmic pathway. *Crit. Rev. Biochem. Mol. Biol.* **34**, 95–106.

Ogura, K. and Koyama, T. (1998) Enzymatic aspects of isoprenoid chain elongation. *Chem. Rev.* **98**, 1263–1276.

Pechous, S.W. and Whitaker, B.D. (2004) Cloning and functional expression of an (*E,E*)-a-farnesene synthase cDNA from peel tissue of apple fruit. *Planta*, **219**, 84–94.

Perkins, D.N., Pappin, D.J., Creasy, D.M. and Cottrell, J.S. (1999) Probability-based protein identification by searching sequence databases using mass spectrometry data. *Electrophoresis*, **20**, 3551–3567.

Pichersky, E., Lewinsohn, E. and Croteau, R. (1995) Purification and characterization of *S*-linalool synthase, an enzyme involved in the production of floral scent in *Clarkia breweri*. *Arch. Biochem. Biophys.* **316**, 803–807.

Poulter, C.D. and Rilling, H.C. (1981) Prenyl transferases and isomerase. In *Biosynthesis of Isoprenoid Compounds*, Vol. 1 (Porter, J.W. and Spurgeon, S.L., eds). New York, NY: John Wiley and Sons, pp. 162–209.

Rodriguez-Concepcion, M. and Boronat, A. (2002) Elucidation of the methylerythritol phosphate pathway for isoprenoid biosynthesis in bacteria and plastids. A metabolic milestone achieved through genomics. *Plant Physiol.* **130**, 1079–1089.

Rohmer, M. (1999) The discovery of a mevalonate-independent pathway for isoprenoid biosynthesis in bacteria, algae and higher plants. *Nat. Prod. Rep.* **16**, 565–574.

van Schie, C.C., Haring, M.A. and Schuurink, R.C. (2007) Tomato linalool synthase is induced in trichomes by jasmonic acid. *Plant Mol. Biol.* **64**, 251–263.

Schnee, C., Köllner, T.G., Gershenzon, J. and Degenhardt, J. (2002) The maize gene *terpene synthase 1* encodes a sesquiterpene synthase catalyzing the formation of (*E*)-beta-farnesene, (*E*)-nerolidol, and (*E,E*)-farnesol after herbivore damage. *Plant Physiol.* **130**, 2049–2060.

Schuhr, C.A., Radykewicz, T., Sagner, S., Latzel, C., Zenk, M.H., Arigoni, D., Bacher, A., Rohdich, F. and Eisenreich, W. (2003) Quantitative assessment of crosstalk between the two isoprenoid biosynthesis pathways in plants by NMR spectroscopy. *Phytochem. Rev.* **2**, 3–16.

Sheen, J. (2002) A transient expression assay using *Arabidopsis* mesophyll protoplasts. Available at http://genetics.mgh.harvard.edu/sheenweb/.

Smith, R.G., Gauthier, D.A., Dennis, D.T. and Turpin, D.H. (1992) Malate and pyruvate dehydrogenase-dependent fatty acid synthesis in leucoplasts from developing castor endosperm. *Plant Physiol.* **98**, 1233–1238.

Steele, C.L., Crock, J., Bohlmann, J. and Croteau, R. (1998) Sesquiterpene synthases from grand fir (*Abies grandis*): comparison of constitutive and wound-induced activities, and cDNA isolation, characterization, and bacterial expression of δ-selinene synthase and γ-humulene synthase. *J. Biol. Chem.* **273**, 2078–2089.

Tholl, D. (2006) Terpene synthases and the regulation, diversity and biological roles of terpene metabolism. *Curr. Opin. Plant Biol.* **9**, 297–304.

Tholl, D., Kish, C.M., Orlova, I., Sherman, D., Gershenzon, J., Pichersky, E. and Dudareva, N. (2004) Formation of monoterpenes in *Antirrhinum majus* and *Clarkia breweri* flowers involves heterodimeric geranyl diphosphate synthases. *Plant Cell*, **16**, 977–992.

Tholl, D., Chen, F., Petri, J., Gershenzon, J. and Pichersky, E. (2005) Two sesquiterpene synthses are responsible for the complex mixture of sesquiterpenes emitted from Arabidopsis flowers. *Plant J.* **42**, 757–771.

Williams, D.C., McGarvey, D.J., Katahira, E.J. and Croteau, R. (1998) Truncation of limonene synthase preprotein provides a fully active 'pseudomature' form of this monoterpene cyclase and reveals the function of the amino-terminal arginine pair. *Biochemistry*, **37**, 12213–12220.

Wise, M.L. and Croteau, R. (1999) Monoterpene biosynthesis. In *Comprehensive Natural Products Chemistry, Vol 2, Isoprenoids Including Carotenoids and Steroids* (Cane, D.D., ed.). Amsterdam: Elsevier Science, pp. 97–153.

Wu, S., Schalk, M., Clark, A., Miles, R.B., Coates, R. and Chappell, J. (2006) Redirection of cytosolic or plastidic isoprenoid precursors elevates terpene production in plants. *Nat. Biotechnol.* **24**, 1441–1447.